

Correlation of atomic packing with the boson peak in amorphous alloys

W. M. Yang, H. S. Liu, X. J. Liu, G. X. Chen, C. C. Dun, Y. C. Zhao, Q. K. Man, C. T. Chang, B. L. Shen, A. Inoue, R. W. Li, and J. Z. Jiang

Citation: *Journal of Applied Physics* **116**, 123512 (2014); doi: 10.1063/1.4896765

View online: <https://doi.org/10.1063/1.4896765>

View Table of Contents: <http://aip.scitation.org/toc/jap/116/12>

Published by the [American Institute of Physics](#)

Articles you may be interested in

[Relationship between boson heat capacity peaks and evolution of heterogeneous structure in metallic glasses](#)
Journal of Applied Physics **115**, 153505 (2014); 10.1063/1.4871676

[High thermal stability and sluggish crystallization kinetics of high-entropy bulk metallic glasses](#)
Journal of Applied Physics **119**, 245112 (2016); 10.1063/1.4955060

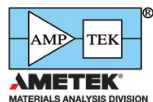
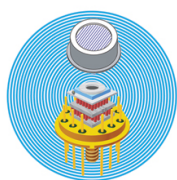
[Universal structural softening in metallic glasses indicated by boson heat capacity peak](#)
Applied Physics Letters **111**, 261901 (2017); 10.1063/1.5016984

[Relaxation in glassforming liquids and amorphous solids](#)
Journal of Applied Physics **88**, 3113 (2000); 10.1063/1.1286035

[Pressure effects on structure and dynamics of metallic glass-forming liquid](#)
The Journal of Chemical Physics **146**, 024507 (2017); 10.1063/1.4973919

[Effect of local structures and atomic packing on glass forming ability in \$\text{Cu}_x\text{Zr}_{100-x}\$ metallic glasses](#)
Applied Physics Letters **96**, 021901 (2010); 10.1063/1.3282800

Ultra High Performance SDD Detectors



See all our XRF Solutions

Correlation of atomic packing with the boson peak in amorphous alloys

W. M. Yang,^{1,2,3} H. S. Liu,^{1,a)} X. J. Liu,⁴ G. X. Chen,² C. C. Dun,⁵ Y. C. Zhao,¹ Q. K. Man,² C. T. Chang,² B. L. Shen,^{3,a)} A. Inoue,^{2,6} R. W. Li,^{2,a)} and J. Z. Jiang^{7,a)}

¹State Key Laboratory for Geomechanics and Deep Underground Engineering, School of Mechanics and Civil Engineering, School of Sciences, China University of Mining and Technology, Xuzhou 221116, People's Republic of China

²Key Laboratory of Magnetic Materials and Devices, Ningbo Institute of Materials Technology & Engineering, Chinese Academy of Sciences, Ningbo 315201, People's Republic of China

³School of Materials Science and Engineering, Southeast University, Nanjing 211189, People's Republic of China

⁴State Key Laboratory for Advanced Metals and Materials, University of Science and Technology Beijing, Beijing 100083, People's Republic of China

⁵Department of Physics, Wake Forest University, Winston-Salem, North Carolina 27109, USA

⁶WPI Advanced Institute for Materials Research, Tohoku University, Sendai 980-8577, Japan

⁷International Center for New-Structured Materials, Zhejiang University, and Laboratory of New-Structured Materials, State Key Laboratory of Silicon Materials, Department of Materials Science and Engineering, Zhejiang University, 310027 Hangzhou, People's Republic of China

(Received 6 July 2014; accepted 18 September 2014; published online 26 September 2014)

Boson peaks (BP) have been observed from phonon specific heats in 10 studied amorphous alloys. Two Einstein-type vibration modes were proposed in this work and all data can be fitted well. By measuring and analyzing local atomic structures of studied amorphous alloys and 56 reported amorphous alloys, it is found that (a) the BP originates from local harmonic vibration modes associated with the lengths of short-range order (SRO) and medium-range order (MRO) in amorphous alloys, and (b) the atomic packing in amorphous alloys follows a universal scaling law, i.e., the ratios of SRO and MRO lengths to solvent atomic diameter are 3 and 7, respectively, which exact match with length ratios of BP vibration frequencies to Debye frequency for the studied amorphous alloys. This finding provides a new perspective for atomic packing in amorphous materials, and has significant implications for quantitative description of the local atomic orders and understanding the structure-property relationship. © 2014 AIP Publishing LLC.

[<http://dx.doi.org/10.1063/1.4896765>]

I. INTRODUCTION

Vibrational dynamics of amorphous solids has been a long-standing subject of experimental, theoretical and computational studies.^{1–15} A universal dynamical feature observed in amorphous solids is that their phonon specific heats, C_{Phonon} , are larger than the predictions of the Debye model with a peak centered at temperatures of 10–30 K in the plot of C_{Phonon}/T^3 vs T , which is called the “boson peak” (BP).^{5–11} After considerable studies, the common belief is that the origin of BP is linked with elastic heterogeneities.^{7–11,15} However, this description has never been quantified partially due to lacking of knowledge of the exact atomic structures for amorphous solids. Thus, it is imperative to find whether there is indeed a relationship of atomic structure in amorphous solids with BP. For this purpose, we carried out specific heats and high resolution transmission electron microscopy (HRTEM) measurements for 10 amorphous alloys. Together with reported pair distribution functions (PDFs) data for 56 amorphous alloys, we provided compelling evidence that BP dynamics strongly correlated with local atomic orders in amorphous alloys.

II. EXPERIMENTAL

Amorphous alloys studied were fabricated using melt-spun or copper-mold casting. Their glassy natures were ascertained by X-ray diffraction (D8 Advance) with Cu K_{α} radiation, differential scanning calorimeter (NETZSCH DSC-404) with a heating rate of 0.67 K/s, and HRTEM using a Tecnai F20 microscope. Image analysis was carried out using the software Gatan Digital Microscopy Suite. The low temperature specific heats for studied amorphous alloys were carried out using the physical property measurement system from quantum design system (Model-9). The final data were obtained by averaging 3 experimental results. The relative error for the specific heat measurements is less than 2%.

III. RESULTS AND DISCUSSION

Figure 1 shows the C_{Phonon}/T^3 vs T for studied amorphous alloys (details for data analyses are given in Figs. S1 and S2, and Table S1 in Supplementary Ref. 16). It has been verified that, in contrast to crystalline solids, the C_{Phonon} of amorphous alloys cannot be described by the Debye model, besides the two-level-systems (TLS) contribution.⁶ Moreover, localized harmonic vibration mode (LHVM) was suggested to exist in amorphous solids.¹⁷ This means an additional Einstein-type vibration also contributes to the

^{a)} Authors to whom correspondence should be addressed. Electronic addresses: liuhaishun@126.com, blshen@seu.edu.cn, runweili@nimte.ac.cn, and jiangzj@zju.edu.cn

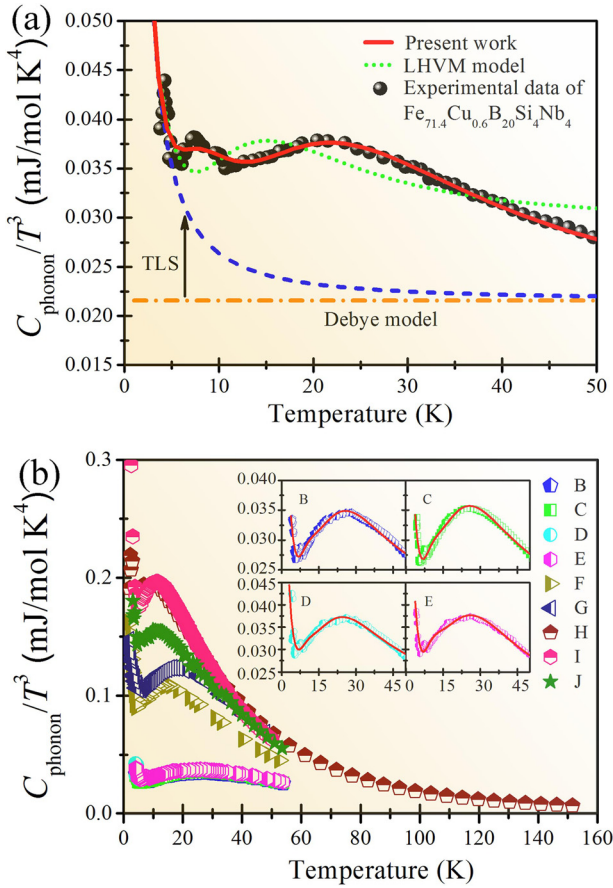


FIG. 1. (a) C_{Phonon}/T^3 vs T for $\text{Fe}_{71.4}\text{Cu}_{0.6}\text{B}_{20}\text{Si}_4\text{Nb}_4$ amorphous alloy. The red solid line through the data is based on a hypothesis that two kinds of Einstein oscillators exist besides Debye oscillators. The green dashed line shows the LHVM model and the blue dashed line shows a sum of the Debye and TLS contribution. (b) C_{Phonon}/T^3 vs T for various amorphous alloys. For clarity, only selected data points are shown. The inset shows the experimental data theoretical lines of Fe-based amorphous alloys in a small range.

C_{Phonon} of amorphous solids, i.e., LHVM with a specific frequency.^{5,18} However, experimental data obtained here and reported data^{19–22} still deviate from theoretical results if only one kind of Einstein-type vibration mode is considered. Thus, here we introduced two kinds of quantized Einstein-type vibration modes to fit the specific heat C_{Phonon} contributed from phonon vibration in amorphous alloys. Somewhat

surprising, good fit to experimental results of 10 studied amorphous alloys are achieved using the proposed two kinds of Einstein-type oscillators. Fig. 1(a) shows a representative fitting result, at which the red line through the data of BP represents a fit to the equation

$$C_{\text{Phonon}} = C_D + \alpha C_{E(B)} + \beta C_{E(C)}, \quad (1)$$

where $C_D = 12\pi^4 R k_B^3 T^3 / 5(\hbar\omega_A)^3$ is the Debye model contribution with a Debye-type vibrational frequency ω_A ; $C_{E(j)} = 3R(\hbar\omega_j/k_B T)^2 e^{\hbar\omega_j/k_B T} / (e^{\hbar\omega_j/k_B T} - 1)^2$ ($j = B$ and C) are the Einstein model contributions with Einstein-type vibrational frequencies ω_B and ω_C , respectively; α and β represent the weight factors of Einstein-type B and C oscillators, respectively. Parameters, ω_A , ω_B , and ω_C as well as α and β , were summarized in Table I. The excellent agreement between theoretical results with the experimental data strongly suggests that two distinct Einstein-type vibration modes exist in amorphous alloys. Furthermore, strong correlations between ω_A and ω_B or ω_C for studied amorphous alloys are detected in Fig. 2 with $\omega_B \approx 0.30 \omega_A$ and $\omega_C \approx 0.15 \omega_A$. According to the localized low frequency dynamics²³ and the Ioffe-Regel condition,²⁴ the vibrational frequency ω is proportional to $1/d$, where d is the diameter of the density fluctuation domains in amorphous solids. The ω decreases with increasing d . Thus, the observed frequency relationships can be expressed as $\omega_A:\omega_B:\omega_C = 1/d_A:1/d_B:1/d_C$, where d_A , d_B , and d_C are corresponding lengths for three local atomic density fluctuation regions, respectively, with $d_A:d_B:d_C \approx 1:3:7$ in studied amorphous alloys.

Despite the lack of long-range crystalline order, amorphous alloys are known to exhibit some degree of short-range order (SRO) and medium-range order (MRO).^{25,26} The SROs are characterized by solute-centered clusters, each of which is made up of a solute atom surrounded by a majority of solvent atoms, and the MROs are constructed by packing of the clusters beyond the SROs. The interaction bonds within SROs and MROs are very strong, while the solvent-solvent bonds linking the SROs and MROs are much weaker,²⁷ the SROs and MROs are suggested vibrate like quasicontinuum regions. Therefore, in macroscopic homogeneous amorphous solids, the density fluctuation domains could exist in different length scales, e.g., atomic, SRO, and

TABLE I. The Debye frequency ω_A , Einstein frequencies ω_B and ω_C for studied amorphous alloys. The parameters α and β are also listed.

| Label | Amorphous alloys | ω_A ($10^{13}/s$) | ω_B ($10^{13}/s$) | ω_C ($10^{13}/s$) | α | β |
|-------|---|----------------------------|----------------------------|----------------------------|----------|---------|
| A | $\text{Fe}_{71.4}\text{Cu}_{0.6}\text{B}_{20}\text{Si}_4\text{Nb}_4$ | 5.864 | 1.749 | 0.715 | 0.045 | 0.0019 |
| B | $(\text{Fe}_{0.9}\text{Co}_{0.1})_{71.4}\text{Cu}_{0.6}\text{B}_{20}\text{Si}_4\text{Nb}_4$ | 6.061 | 1.881 | 0.835 | 0.059 | 0.0037 |
| C | $(\text{Fe}_{0.7}\text{Co}_{0.3})_{71.4}\text{Cu}_{0.6}\text{B}_{20}\text{Si}_4\text{Nb}_4$ | 6.165 | 1.950 | 0.890 | 0.063 | 0.0042 |
| D | $(\text{Fe}_{0.5}\text{Co}_{0.5})_{71.4}\text{Cu}_{0.6}\text{B}_{20}\text{Si}_4\text{Nb}_4$ | 6.179 | 1.785 | 0.801 | 0.072 | 0.0046 |
| E | $(\text{Fe}_{0.3}\text{Co}_{0.7})_{71.4}\text{Cu}_{0.6}\text{B}_{20}\text{Si}_4\text{Nb}_4$ | 6.283 | 1.873 | 0.812 | 0.074 | 0.0054 |
| F | $\text{Zr}_{46.75}\text{Ti}_{8.25}\text{Cu}_{7.5}\text{Ni}_{10}\text{Be}_{27.5}$ | 3.338 | 1.133 | 0.457 | 0.062 | 0.0030 |
| G | $\text{Zr}_{52.5}\text{Cu}_{17.9}\text{Ni}_{14.6}\text{Al}_{10}\text{Ti}_5$ | 4.176 | 1.157 | 0.474 | 0.269 | 0.0188 |
| H | $\text{Pd}_{41.25}\text{Cu}_{41.25}\text{P}_{17.5}$ | 3.011 | 0.903 | 0.392 | 0.105 | 0.0097 |
| I | $\text{Cu}_{50}\text{Zr}_{50}$ | 3.809 | 1.051 | 0.400 | 0.050 | 0.0007 |
| J | $(\text{Cu}_{0.5}\text{Zr}_{0.5})_{93}\text{Al}_7$ | 3.796 | 1.178 | 0.508 | 0.233 | 0.0263 |
| K | $^a\text{Cu}_{60}\text{Zr}_{20}\text{Hf}_{10}\text{Ti}_{10}$ | 4.333 | 1.479 | 0.537 | 0.240 | 0.0433 |

^aReference 20.

MRO lengths. Here, we proposed that d_A , d_B , and d_C could be corresponded to the lengths of solvent atomic size, SRO and MRO lengths in amorphous solids, respectively. To support this scenario, we performed atomic structure measurements using HRTEM. From the obtained experimental atomic structure results together with reported structural data for 56 amorphous alloys, strong correlations of SRO and MRO lengths with BP vibration frequencies are indeed detected. Details are explained in the following section.

In order to determine what kind of oscillators contribute to the boson peak, we first compared ω_A for 30 amorphous alloys and their solvent metals (Table S2 and Fig. S3). It is found that Debye frequencies of many amorphous alloys are very close to their base atoms (or solvent atoms). This reveals that the Debye-type specific heats of amorphous alloys are mainly contributed from the solvent atoms, which results in d_A might be close to the average diameter of solvent atoms, d_S . Second, we focus on the lengths of SRO and MRO for amorphous alloys by HRTEM, which is one of effective tools to get atomic scale information.²⁸ As an example, Fig. 3 shows local atomic order ranges in a $\text{Fe}_{71.4}\text{Cu}_{0.6}\text{B}_{20}\text{Si}_4\text{Nb}_4$ amorphous alloy. Fig. 3(b) shows fast Fourier transform (FFT) and corresponding inverse fast Fourier transform (IFFT) for a randomly selected area. The inset also shows a typical amorphous pattern, even though the atom-centered clusters (SRO regions) and five-fold symmetry superclusters (MRO regions) are marked by circles in image from IFFT. To have a quantitative description of the length scales of local atomic order, the statistical analysis was carried out by analyzing more than 100 spots from a large number of IFFT images (Figs. 3(c)–3(g)). It is found that the SRO and MRO lengths are about 0.75 nm and 1.75 nm, respectively, very close to 3 and 7 times of solvent Fe atomic size (0.247 nm) in $\text{Fe}_{71.4}\text{Cu}_{0.6}\text{B}_{20}\text{Si}_4\text{Nb}_4$ amorphous alloy. For amorphous alloys, as discussed by Suzuki *et al.*²⁹ and Wanger *et al.*,³⁰ the peaks in pair distribution function, $g(r)$, describe the SRO and MRO regions in real space, while the first strong peak at r_1 corresponds to the average distance between the first nearest-neighbor shell and centered (solvent) atoms, $r_A \approx d_A$. For the shell number

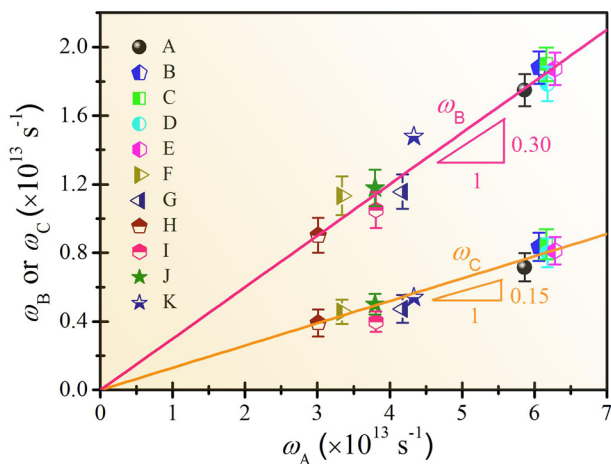


FIG. 2. The relationship among ω_A , ω_B , and ω_C for various amorphous alloys. The solid lines represent linear fits to the data.

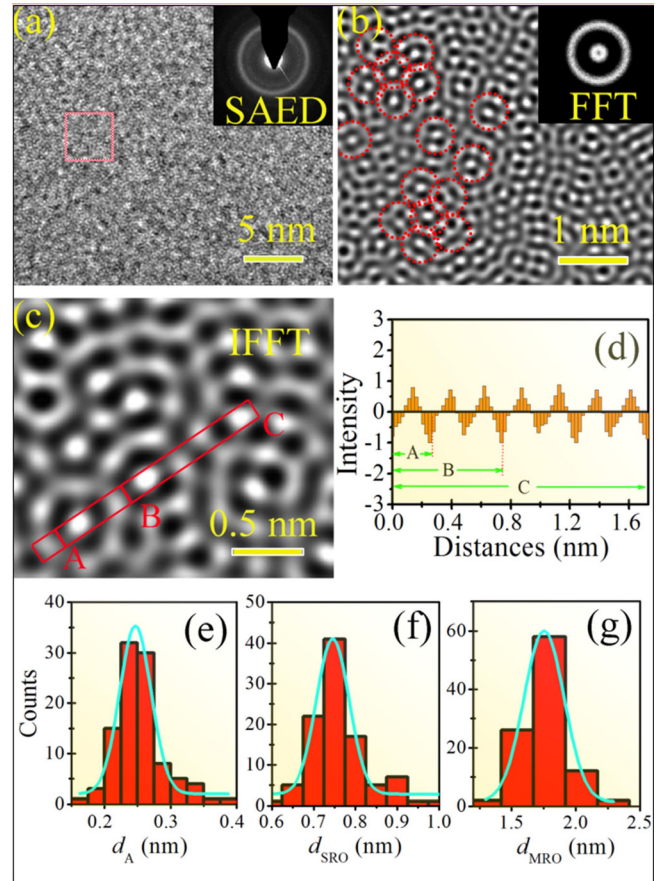


FIG. 3. (a) HRTEM image and corresponding SAED pattern of the cast $\text{Fe}_{71.4}\text{Cu}_{0.6}\text{B}_{20}\text{Si}_4\text{Nb}_4$ amorphous alloy. (b) The FFT and IFFT patterns for the randomly selected area marked by a red line square ($4 \times 4 \text{ nm}^2$) in (a). (c) A typical IFFT pattern obtained from $\text{Fe}_{71.4}\text{Cu}_{0.6}\text{B}_{20}\text{Si}_4\text{Nb}_4$ amorphous alloy. (d) The intensity profile along the arrow of a typical IFFT pattern is obtained from $\text{Fe}_{71.4}\text{Cu}_{0.6}\text{B}_{20}\text{Si}_4\text{Nb}_4$ in (c), which can be used to measure interatomic spacings. (e)–(g) The statistics of interatomic spacings measured from more than 100 spots for single atom, SRO, and MRO lengths in HRTEM images, respectively.

$i > 6$, it has been verified $g(r_i) \rightarrow 1$ correspondingly for most amorphous alloys.^{29–31} Recently, Liu *et al.* revealed that the atomic packing in amorphous alloys can be described globally by the spherical-periodic orders.^{32,33} Based on above considerations, the SRO and MRO lengths can be regarded as diameters for spheres, which have the diameters of $d_{\text{SRO}} = 2r_B$ for SRO and $d_{\text{MRO}} \approx 2r_C$ for MRO,^{34,35} as illustrated in Fig. 4(a). The decisive length scales of SRO and MRO from PDFs of reported 56 amorphous alloys (in Table S3) are estimated about 0.73–0.94 nm and 1.70–2.10 nm, respectively, which agrees with the direct observation results.²⁸ Fig. 4(b) shows the statistical results of the ratio of d_S , d_{SRO} , and d_{MRO} to r_A for 56 amorphous alloys. All the data points fall on three lines, despite of the diversity of samples including both pure metals and amorphous alloys. Thus, the d_S , d_{SRO} , and d_{MRO} are approximately 1, 3, and 7 times of d_A or (r_A), respectively. This result further demonstrates the universal scaling law that the length scales of SROs and MROs are approximately 3 and 7 times of the diameter of solvent atoms in amorphous alloys, respectively, which exactly match with the corresponding lengths for BP

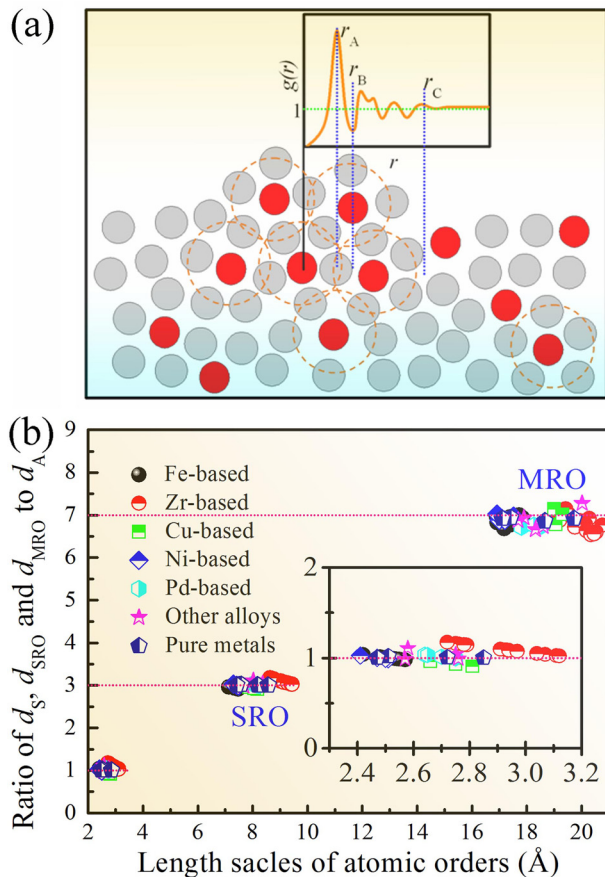


FIG. 4. (a) Schematic illustration of the structural origin of certain features in the pair distribution function of amorphous alloys. (b) Ratios of d_S , d_{SRO} , and d_{MRO} to d_A for 56 amorphous alloys ranging from single to quinary systems. The inset shows the ratio of d_S to d_A in a small range. The red dashed lines are drawn to guide the eyes.

vibration frequencies in amorphous alloys. This correlation can be understood as follows.

The SROs are used to avoid forming nucleus of crystallographic phases in amorphous solids.³⁶ To achieve the thermodynamical equilibrium state with lower free energy and fill space, some of the SROs are also tightly connected surrounding a solute atom, as they share solvent atoms at vertices, edges or faces, to form the five-fold symmetry MROs in amorphous alloys. The regions between SROs and/or MROs might be empty or occupied by lone solvent atoms that do not form clusters. However, such kind of local atomic arrangement cannot continue to form the long-range orders beyond the length scale of a few clusters, owing to the five-fold symmetry and structural aberration from chemical and topological order.³⁷ In other words, the SROs and MROs in amorphous structure are formed in the supercooled melt and their length scales have no detectable relationship with the process of vitrification.^{38,39} Furthermore, densities for most amorphous alloys are only 0.5%–3% less than the values for corresponded crystalline alloys, indicating free volume (or open volume) does exist in amorphous alloys. Based on considerable structure investigations, it is accepted to believe that amorphous alloys are composed of atomic clusters with a similar SRO length or even superclusters with a similar MRO length.^{25–27,37} The atomic interactions within SRO

clusters and MRO superclusters are stronger while the atomic interactions linking the SRO clusters and MRO superclusters, where high open volumes may have, are weaker. Therefore, the SRO length-sized clusters and MRO length-sized superclusters in amorphous alloys could vibrate like quasi-continuum regions and result in the localized harmonic modes for the BP peak.

IV. CONCLUSIONS

In summary, BPs have been observed in 10 studied amorphous alloys, which are fitted to two Einstein-type vibration modes. By measuring and analyzing local atomic structures of studied amorphous alloys and 56 reported amorphous alloys, it is found that the ratios of SRO and MRO lengths to solvent atomic diameter are 3 and 7, respectively, which exact match with length ratios of BP vibration frequencies to Debye frequency for the studied amorphous alloys. These results reveal the relationship of BP with SROs and MROs in amorphous alloys and, also quantitatively characterize the local atomic orders, which may provide a feasible way to understand the local atomic orders in amorphous solids.

ACKNOWLEDGMENTS

We thank Dr. K. Zhang, and Dr. S. P. Pan for the contribution to the data. Insightful discussions with Professor H. Schober are also appreciated. This work was supported by the Natural Science Foundation of Jiangsu Province (No. BK20141124), the National Basic Research Program of China (No. 2012CB825700), the National Natural Science Foundation of China (Nos. 51271194, 51271212, and 51323004).

- ¹S. R. Elliott, *Physics of Amorphous Materials* (Wiley, New York, 1984).
- ²W. Kob and K. Binder, *Glassy Materials and Disordered Solids: An Introduction* (World Scientific, London, 2011).
- ³U. Buchenau *et al.*, *Phys. Rev. Lett.* **53**, 2316 (1984).
- ⁴M. B. Tang, J. Q. Wang, and W. H. Wang, *et al.*, *J. Appl. Phys.* **108**, 033525 (2010).
- ⁵B. B. Laird and H. R. Schober, *Phys. Rev. Lett.* **66**, 636 (1991).
- ⁶A. P. Sokolov *et al.*, *Phys. Rev. Lett.* **78**, 2405 (1997).
- ⁷W. Schirmacher, G. Diezemann, and C. Ganter, *Phys. Rev. Lett.* **81**, 136 (1998).
- ⁸W. Goetze and M. R. Mayr, *Phys. Rev. E* **61**, 587 (2000).
- ⁹J. W. Kantelhardt, S. Russ, and A. Bunde, *Phys. Rev. B* **63**, 064302 (2001).
- ¹⁰W. Schirmacher, G. Ruocco, and T. Scopigno, *Phys. Rev. Lett.* **98**, 025501 (2007).
- ¹¹H. Shintani and H. Tanaka, *Nature Mater.* **7**, 870 (2008).
- ¹²G. Monaco and V. M. Gordano, *Proc. Natl. Acad. Sci. U.S.A.* **106**, 3659 (2009).
- ¹³G. Baldi *et al.*, *Phys. Rev. Lett.* **104**, 195501 (2010).
- ¹⁴B. Ruta *et al.*, *J. Chem. Phys.* **133**, 041101 (2010).
- ¹⁵A. Marruzzo *et al.*, *Sci. Rep.* **3**, 1407 (2013).
- ¹⁶See supplemental material at <http://dx.doi.org/10.1063/1.4896765> for details of experiments and data analysis.
- ¹⁷A. V. Granato, *Physica B* **219–220**, 270 (1996).
- ¹⁸Y. Li *et al.*, *Phys. Rev. B* **74**, 052201 (2006).
- ¹⁹M. B. Tang *et al.*, *Appl. Phys. Lett.* **86**, 021910 (2005).
- ²⁰A. N. Vasiliev *et al.*, *Phys. Rev. B* **80**, 172102 (2009).
- ²¹M. B. Tang, H. Y. Bai, and W. H. Wang, *Phys. Rev. B* **72**, 012202 (2005).
- ²²Z. X. Wang, B. Sun, and J. B. Lu, *Trans. Nonferrous Met. Soc. China* **21**, 1309 (2011).
- ²³T. Uchino and T. Yoko, *J. Chem. Phys.* **108**, 8130 (1998).

- ²⁴S. R. Elliott, *Europhys. Lett.* **19**, 201 (1992).
- ²⁵D. B. Miracle, *Nature Mater.* **3**, 697 (2004).
- ²⁶H. W. Sheng *et al.*, *Nature (London)* **439**, 419 (2006).
- ²⁷D. Ma, *et al.*, *Phys. Rev. Lett.* **108**, 085501 (2012).
- ²⁸A. Hirata *et al.*, *Nature Mater.* **10**, 28 (2011).
- ²⁹Y. Suzuki, J. Haimovich, and T. Egami, *Phys. Rev. B* **35**, 2162 (1987).
- ³⁰C. N. Wanger *et al.*, *J. Appl. Phys.* **39**, 3690 (1968).
- ³¹K. Zhang *et al.*, *Appl. Phys. Lett.* **102**, 071907 (2013).
- ³²X. J. Liu *et al.*, *Phys. Rev. Lett.* **105**, 155501 (2010).
- ³³X. J. Liu *et al.*, *Acta Mater.* **59**, 6480 (2011).
- ³⁴A. I. Oreshkin *et al.*, *Acta Mater.* **61**, 5216 (2013).
- ³⁵X. W. Fang *et al.*, *Sci. Rep.* **1**, 194 (2011).
- ³⁶Y. Q. Cheng *et al.*, *Phys. Rev. Lett.* **102**, 245501 (2009).
- ³⁷D. Ma, A. D. Stoica, and X. L. Wang, *Nature Mater.* **8**, 30 (2009).
- ³⁸V. K. Malinovsky and A. P. Sokolov, *Solid State Commun.* **57**, 757–761 (1986).
- ³⁹V. K. Malinovsky, A. P. Novikov, and A. P. Sokolov, *Phys. Lett. A* **123**, 19–22 (1987).